The accuracy of image-based safety analysis for robotic cochlear implantation

C. Rathgeb, F. Wagner, W. Wimmer, N. Gerber, T. Williamson, L. Anschütz, S. Weder, M. Stadelmann, G. Braga, J. Anso, M. Caversaccio, et al.

International Journal of Computer Assisted Radiology and Surgery
A journal for interdisciplinary research, development and applications of image guided diagnosis and therapy

ISSN 1861-6410

Int J CARS
DOI 10.1007/s11548-018-1834-3

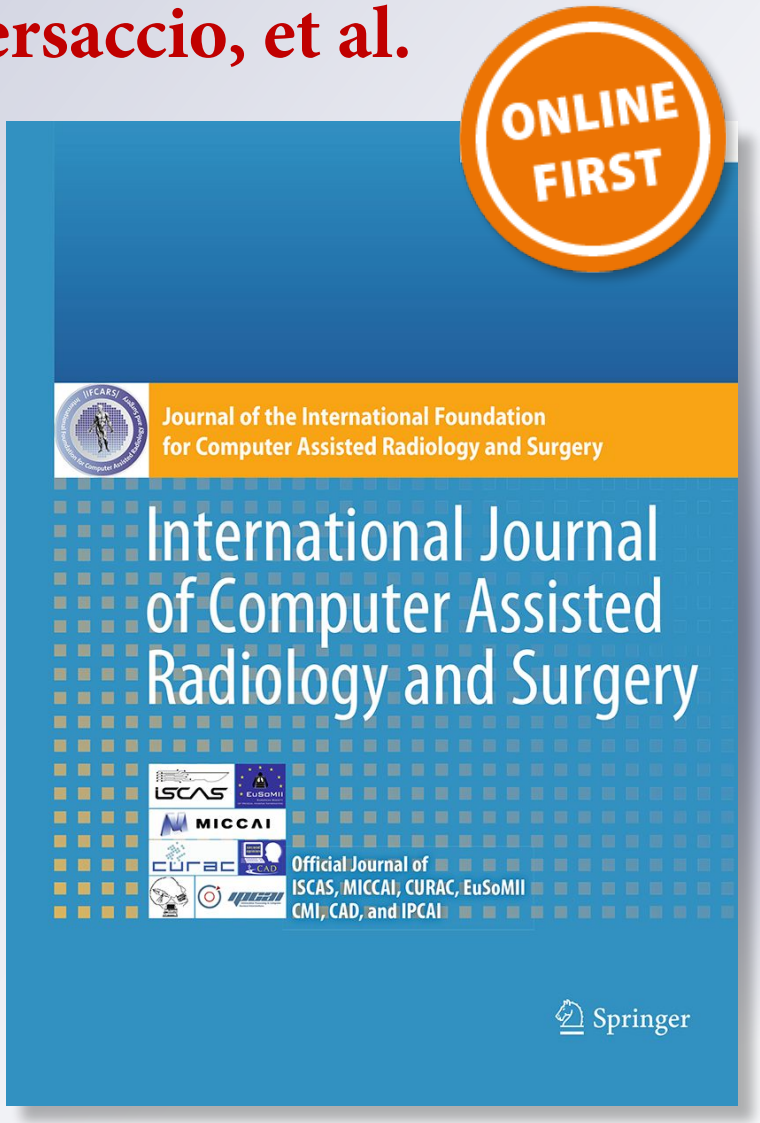

Springer

International Journal of Computer Assisted Radiology and Surgery
https://doi.org/10.1007/s11548-018-1834-3

ORIGINAL ARTICLE

The accuracy of image-based safety analysis for robotic cochlear implantation

C. Rathgeb[1] · F. Wagner[2] · W. Wimmer[1,3] · N. Gerber[4] · T. Williamson[4] · L. Anschütz[3] · S. Weder[3] · M. Stadelmann[5] · G. Braga[4] · J. Anso[4] · M. Caversaccio[1,3] · S. Weber[4] · K. Gavaghan[4]

Received: 10 April 2018 / Accepted: 26 July 2018

Abstract

Purpose To evaluate the accuracy and reliability of image-based safety analysis for robotic cochlear implantation (RCI) in an ex vivo assessment.

Methods The accuracy was evaluated in a study on 23 human temporal bones. For image analysis, a computer-assisted safety analysis based on intraoperative cone beam computed tomography was implemented. The method automatically segments the drill tunnel and predicts the distance between the tunnel and the facial nerve. In addition, the drilling error at the target is predicted. The predicted distances were compared with the actually drilled distances measured in postoperative high-resolution micro-computed tomography scans. The automatic method was compared to accuracies associated with a manual analysis of the image data.

Results The presented computerized image-based analysis enabled the proximity of the facial nerve to the drill trajectory to be predicted with an accuracy of 0.22 ± 0.15 mm and drilling error at the target to be predicted with an accuracy of 0.11 mm ± 0.08 during $N = 19$ RCI procedures. The manual assessment of facial nerve proximity was performed with an accuracy of 0.34 ± 0.20 mm by a trained clinical expert.

Conclusion The assessment of intraoperative CT-based imaging presents multiple benefits over alternative safety mechanisms including early detection and applicability even in cases of malformation of the mastoid. This work presents a computer-assisted approach to image analysis that enables procedure safety measurements to be reliably performed with superior accuracy to other proposed safety methodologies, at a safe distance from the facial nerve. Its application must, however, be considered in relation to associated costs (time, cost, irradiation) and the dependence of the measure on a reliable preoperative segmentation.

Keywords Robotic cochlear implantation · Intraoperative imaging · Safety mechanism

Introduction

Cochlear implants (CIs) are used to restore hearing in the case of profound to severe hearing loss. Their implantation involves the insertion of an electrode array into the cochlea, situated at an approximate depth of 30 mm in the mastoid bone of the skull. A novel, robotically assisted CI implantation procedure (robotic cochlear implantation, RCI) in which access to the cochlea is gained via a minimally invasive tunnel has recently been introduced by Caversaccio et al. [1]. The procedure involves the image-guided robotic drilling of an access tunnel from the surface of the mastoid to the inner ear. Due to close-lying microanatomy, the access tunnel is often planned within a millimeter of critical structures such as the facial nerve. Thus, the procedure requires high levels of

✉ W. Wimmer
wilhelm.wimmer@artorg.unibe.ch

1 Hearing Research Laboratory, ARTORG Center for Biomedical Engineering Research, University of Bern, Bern, Switzerland

2 Department of Diagnostic and Interventional Neuroradiology, Inselspital, University Hospital, University of Bern, Bern, Switzerland

3 Department of Otorhinolaryngology, Head and Neck Surgery, Inselspital, University Hospital, University of Bern, Bern, Switzerland

4 Image Guided Therapy, ARTORG Center for Biomedical Engineering Research, University of Bern, Bern, Switzerland

5 Institute for Surgical Technology and Biomechanics, University of Bern, Bern, Switzerland

Published online: 02 August 2018

navigation accuracy and additional independent tool position and orientation verification methodologies. The dedicated computed tomography (CT)-based image guidance system described by Caversaccio et al. [1] and Weber et al. [2] has demonstrated a high level of tool positioning accuracy and precision (0.15 ± 0.08 mm at the level of the cochlea) [3]. Additionally, a number of methods for confirming the safety of close-lying critical anatomy and particularly the facial nerve have also been proposed. Methods utilizing sensed process signals, including the estimation of drill position and orientation based on the correlation of drilling forces and bone density [4], and methods based on sensed biological signals, such as facial nerve electromyography [5] for facial nerve proximity determination, have been proposed and clinically applied.

Force-based instrument tracking provides an accurate and independent measure of drill position and orientation intraoperatively. The algorithm can determine accuracy of the tunnel placement and predict safety margins between the drill tunnel and the proximal anatomical structures on reaching the depth of the facial nerve with an accuracy of 0.38 ± 0.16 mm [4]. However, because the algorithm relies on variation in mastoid density, the reliability and effectiveness of the drill position and orientation calculation are anatomy specific. The safety algorithm is also not applicable in certain cases (e.g., ossification of the mastoid), and a reliable measure of safety calculation confidence, indicating cases in which the algorithm is applicable or not, is not yet available [4]. Facial nerve electromyography is commonly used for the detection of facial nerve proximity in conventional cochlear implantation surgery. Specialized systems and protocols enabling high-specificity measurements can be employed to reliably prevent mechanical penetration of the nerve during the robotic approach [5]. However, while recent findings indicate that it can be used to warn of an impending breach into the facial nerve canal, the proximity of the warning (less than 0.1 mm from the nerve) may not prevent thermal damage to the nerve. It has thus been recommended to be used in conjunction with additional safety features.

Medical imaging has long been utilized in other surgical domains to assess the location of an inserted instrument intraoperatively. Primarily, instrument locations relative to anatomical structures of interest are determined via visual inspection of the image data and the use of general measurement tools. Within the first clinical cases of a template-based tunnel approach to the cochlea, Labadie et al. utilized portable cone beam computed tomography (CBCT) imaging to assess the safety of the drill trajectory [6]. While they demonstrated the feasibility of employing intraoperative imaging during the procedure, a standardized methodology for assessing the images and validation of the accuracy of the assessment methodology is yet to be reported. With such small margins between the drill tunnel and the facial nerve (0.2–1 mm), distances to be measured on intraoperative images are similar to available image voxel sizes (0.1–0.3 mm), rendering a reliable calculation using traditional manual measurement tools challenging. The need for an intraoperative analysis, performed after a partial drilling of the access tunnel, prior to reaching the depth of the close-lying critical anatomy complicates the task further. It requires the final drill path to be predicted from the partially drilled access tunnel visible in the intraoperative image. Additionally, the closest point on the surface of the nerve, by which this predicted tunnel will pass, must also be identified, even before a distance measure can be obtained.

While medical imaging is a valuable assessment tool that provides a three-dimensional view of the underlying surgical situation, the accuracy of the assessment is currently unknown. Knowledge of the accuracy of a safety methodology is paramount not only to enabling surgeons to successfully evaluate and apply the result of the safety analysis during the procedure, but also to the general definition of required procedure safety margins. Additionally, the accuracy and reliability of a safety methodology can be used to define a hierarchy of safety metrics when multiple safety methodologies (possibly presenting conflicting results) are employed.

Within this work, we aimed to quantify the accuracy of image-based safety analysis for robotic cochlear implantation. To overcome challenges pertaining to manual safety measures, a computer-assisted approach to the analysis of the image data is presented. The associated accuracy of the presented approach was determined in an ex vivo study on human temporal bones along with the accuracy associated with the traditional manual assessment of image data.

Materials and methods

A computer-assisted safety analysis based on CBCT intraoperative images was developed for the existing RCI system described by Caversaccio et al. [1] and Weber et al. [2]. The associated accuracy of the analysis, in determining the location of the drill tunnel, at a safe drilling depth, was assessed along with the accuracy of a traditional manual image-based assessment. The safety analyses methodologies were applied in RCI procedures performed on human temporal bone specimen. The accuracy of calculated safety metrics was computed from ground-truth postoperative values determined from high-resolution image data of the completely drilled access tunnel.

Robotic access to the inner ear

The robotic system, previously described in detail [1, 2, 7], utilizes the registration of bone-anchored fiducial screws,

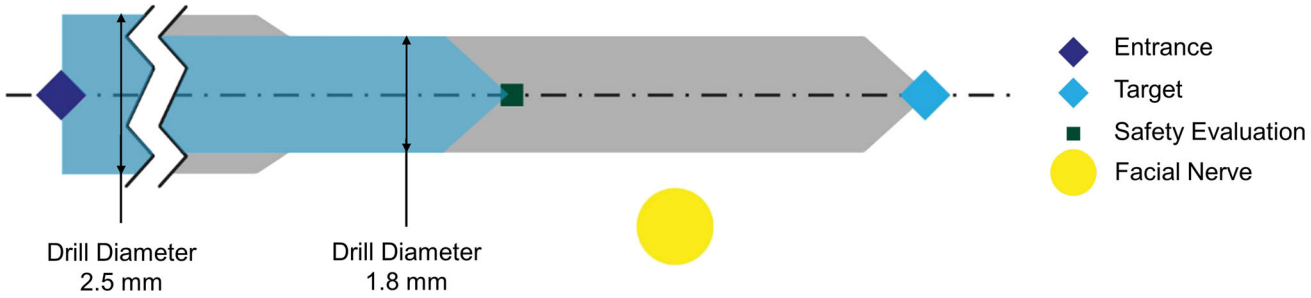

Fig. 1 Overview of planned drill trajectory. The intraoperative safety evaluation point is defined before the level of the facial nerve

high-resolution preoperative CT-based planning and high-accuracy optical tracking of the patient and end effector to drill a preoperatively planned access to the inner ear. Custom planning software provides automatic and semiautomatic algorithms for the localization of the fiducial screws in the image and segmentation of the surrounding critical anatomy (external ear canal, chorda tympani, facial nerve and ossicles) [8]. A target drilling position is selected on the cochlea, and a drill trajectory is defined from the segmented surface of the mastoid bone. The planned trajectory is drilled based on optical tracking of the drill relative to the patient and pair point matching registration of the implanted fiducials.

To allow for image-based assessment of the drill trajectory during the procedure at a safe distance from critical structures, the planning software was augmented to calculate a patient-specific safety evaluation point along the planned trajectory 3 mm from the segmented facial nerve [9] (Fig. 1). The safety evaluation point was defined as 3 mm prior to the closest point on the segmented facial nerve to the planned trajectory projected to the centerline of the planned trajectory. The location of the safety evaluation point was defined to optimize image analysis accuracy while ensuring sufficient distance to prevent injury to the facial nerve in case of drill-positioning error in direction of the tool axis.

On automatic detection of the drill tip reaching the defined safety evaluation point during the procedure, the robotic system interrupts the drilling process and moves away from the surgical site. A custom radio-translucent carbon fiber head clamp (utilizing inflatable pads for head stabilization) allows imaging of the patient's head without the need for repositioning. The patient optical reference, anchored to the mastoid with a single screw, is removed intraoperatively prior to imaging and replaced after the image-based assessment to minimize artifact in the image data. A three-dimensional image dataset of the patients head is acquired after draping the surgical site. To enhance contrast of the drill tunnel in the intraoperative image and to remove effects of air cells on the edge of the drilled tunnel, a cylindrical two-step titanium rod (titanium alloy, Ti–6Al–4V Grade 5) with the same dimensions of the drill bit (2.5 mm diameter, 25 mm length shaft and 1.8 mm diameter, 10 mm tip) was inserted into the robotically drilled tunnel for imaging.

Computer-assisted image analysis

While manual assessment of image data has focused on the determination of the proximity of the most critical proximal structure, the facial nerve, computer-assisted analysis additionally enables the drilling accuracy relative to the planned trajectory to be calculated. A computer-assisted approach to the calculation of nerve proximity and drilling error was developed based on template-based segmentation of the drill tunnel and alignment of the preoperatively defined drill tunnel and anatomical structures to the intraoperative image data. The approach involves three primary steps: drill tunnel segmentation, drill tunnel prediction and distance calculations (Fig. 2).

Drill tunnel segmentation

Using the insight segmentation and registration toolkit (ITK), the drilled tunnel is automatically localized in the intraoperative image using a model-based structure identifier to determine the position and orientation of the inserted titanium rod (Fig. 3), similar to that described by Gerber et al. [9]. The rod is coarsely located in the intraoperative image via the application of a threshold filter for high intensity in the range of titanium (>2500 HU), followed by a region connection filter. It is then distinguished from the fiducial screws and noise using volume information.

The binary image is cropped around the rod, and a mask is generated using a connected threshold region growing, which is initiated at the centroid of the coarsely defined rod. From the binary subvolume, the vertices on the surface of the rod are extracted with a gradient magnitude-based method. A coarse registration of a 3D computer-aided design (CAD) surface model of the rod to the corresponding surface extracted from the image is computed using their respective centroids and principal axes. An iterative closest point matching algorithm is then used along with a *k–d* tree structure to iteratively match the 3D model surface points to the image-extracted

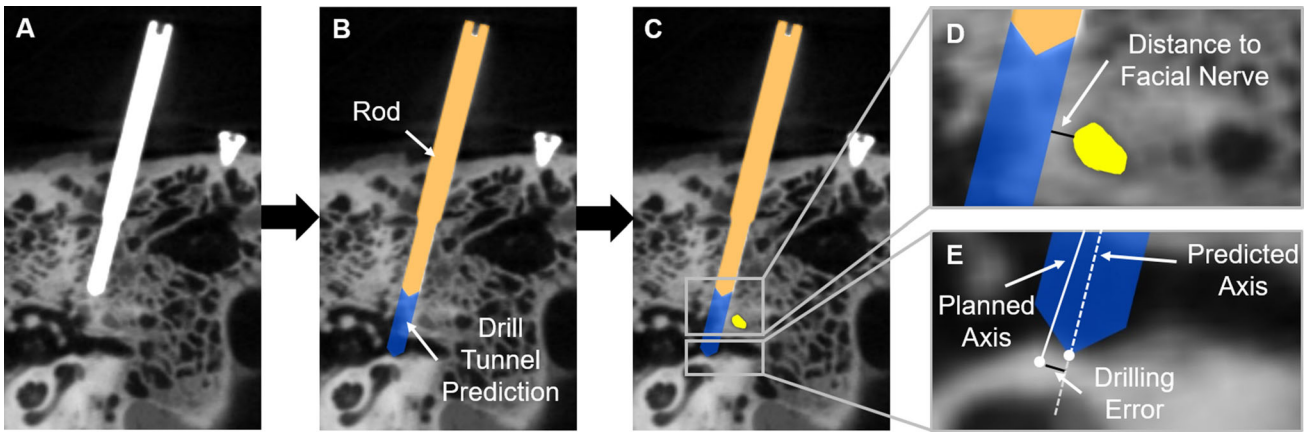

Fig. 2 Overview of computer-assisted image-based safety analysis. **a** Input image with titanium rod. **b** Drill tunnel segmentation and drill tunnel prediction. **c** Distance calculations: facial nerve proximity and drilling error. **d** Calculation of shortest distance between the facial nerve and the predicted drill tunnel. **e** Calculation of target drilling error

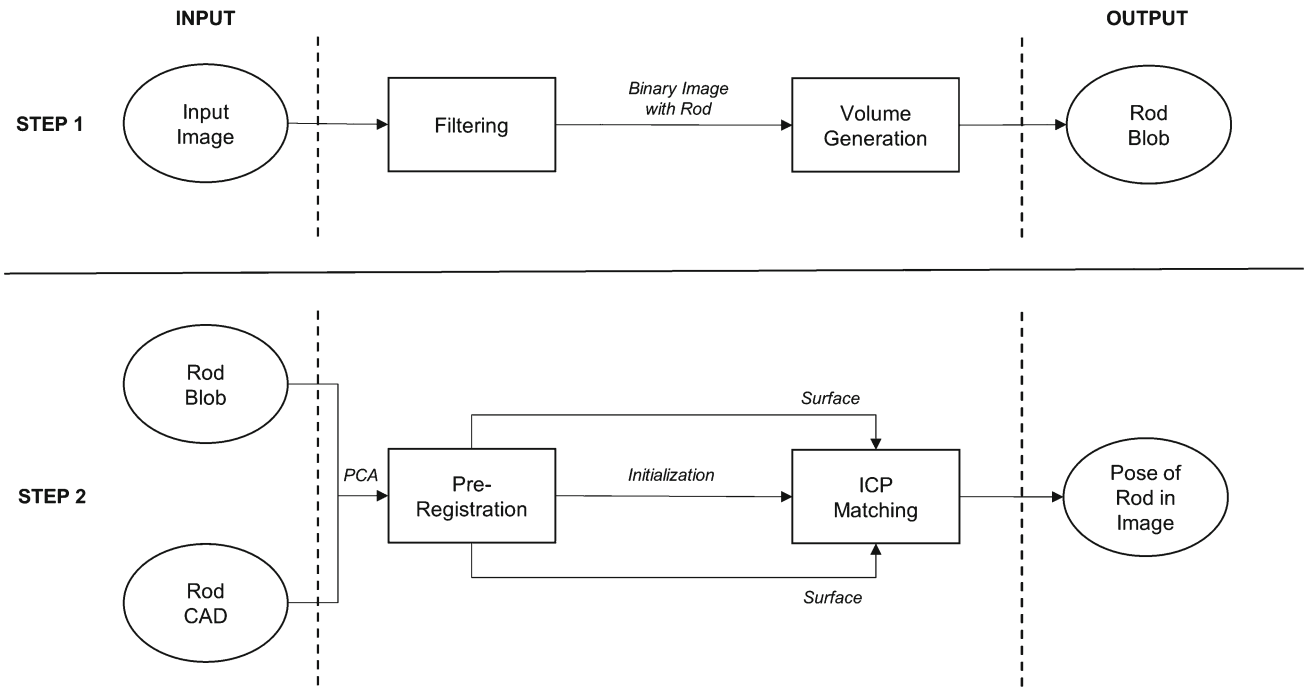

Fig. 3 Drill tunnel segmentation. Step 1 requires an image containing the rod as input and outputs a 3D blob of the rod. The 3D blob of the rod is generated by applying different filters and a region growing algorithm. Step 2 takes the rod blob and the rod CAD model as input and outputs the pose of the CAD rod model within the image. An ICP matching algorithm (initialized through a preregistration step) aligns the rod CAD model with the rod blob using both surfaces

surface. Finally, the estimated position and orientation of the CAD rod model are transformed into the image coordinate system.

Drill tunnel prediction

From the fitted titanium rod model, the position and the axis of the drilled tunnel are extracted. The axis is extended from the tip beyond the level of the facial recess to the depth of the planned drilling target based on the initial length of the planned trajectory. A prediction of the final two-step drill tunnel is then determined by positioning the rod model along the extended axis with its tip at the depth of the planned robotic drilling target.

Distance calculations

The anatomical models segmented from the preoperative CT data and the planned trajectory model are transformed into the intraoperative image coordinate system using a two-stage coarse-to-fine rigid registration algorithm. The data are initially aligned via pair point matching of the preoperative and intraoperative fiducial screw positions, which are automatically located by the planning software using the algorithm described by Gerber et al. [9]. To correct for error caused by reduced resolution of the intraoperative image, a fine registration is then computed using an image-to-image registration with a normalized mutual information metric [10]. Facial nerve proximity is calculated as the shortest distance between the transformed preoperative facial nerve surface model and the drill tunnel prediction model. The distance between the predicted tunnel and the planned tunnel at the depth of the planned target location on the cochlear is calculated as the drilling error.

Accuracy evaluation

The safety prediction accuracy of both manual and computer-assisted image-based safety analysis was assessed in an experiment performed on human cadaveric temporal bone specimen.

Sample preparation and surgical planning

The ex vivo study was approved by the local ethical committee (KEK-BE 2016-00887). Fifteen formalin- and eight thiel -fixed human temporal bones were prepared with four fiducial titanium screws (2.2 mm $\times$ 5 mm length, M-5243.05, Medartis, Switzerland) for patient-to-image registration during robotic direct cochlear access tunnel drilling [1]. Preoperative CT images ($0.15 \times 0.15 \times 0.2$ mm^3, 94 mA, 120 kV, SOMATOM Definition Edge, Siemens, Germany) were acquired, and the facial nerve, chorda tympani, ossicles and external ear canal were segmented using the software described by Gerber et al. [9]. A tunnel through the facial recess targeting the center of the round window membrane was planned. Based on the drilling accuracy of the used robotic system and risk to the facial nerve due to mechanical and thermal exposure, typically a planned safety margin of 0.3 mm to the facial nerve is recommended for RCI drilling [11, 12]. Within this study, however, trajectories passing within closer proximity to the facial nerve were included.

Robotic drilling

With the robotic system in place, a first segment starting at the mastoid surface to the predefined intraoperative evaluation point 3 mm from the facial nerve was drilled using the standard RCI drilling protocol [2] (Fig. 4). CBCT images were acquired (0.3 mm isotropic, 6 mA, 120 kV, xCAT, Xoran, USA) with the patient optical reference removed and the titanium rod inserted into the drilled tunnel. As in clinical implementation, the titanium rod was inserted until significant resistance was experienced. Image quality was visually confirmed on the CBCT imaging system for sufficient contrast and sharp edges of the implanted fiducial screws and the rod.

Computer-assisted and manual safety analysis of the CBCT data as described below was performed, and the time required for assessment was recorded. After reattachment of the patient optical reference and removal of the titanium rod, the RCI access drilling was completed to the inner ear after repetition of the patient-to-image registration.

Computer-assisted image analysis

For each case of RCI drilling, a computer-assisted safety analysis based on the acquired CBCT image dataset was performed. Utilizing the presented computer-assisted safety methodology, the proximity at which each drill trajectory would pass by the facial nerve was predicted based on the aligned preoperatively segmented facial nerve. Additionally, drilling error at the depth of the planned target on the round window membrane relative to the planned drill trajectory was automatically calculated.

Manual image analysis

In addition to the computer-assisted analysis, manual analysis of the intraoperatively acquired CBCT image data was performed. A neuroradiologist trained and experienced in RCI manually predicted the distance at which the drill tunnel would pass the facial nerve on the intraoperative images using clinically available standard clinical visualization tools (Sectra PACS, Sweden). For the manual evaluation of the image data, the neuroradiologist was not informed of the preoperatively planned distance from the drill tunnel to the facial nerve or the automatically calculated distances. On each image dataset, the distance was estimated using the following process: reslicing the image dataset along the approximate axis of the inserted rod, localization of the facial nerve, drill path prediction and closest distance estimation using standard integrated ruler tools (Fig. 5).

Postoperative analysis

Postoperatively each specimen underwent high-resolution imaging (0.06 mm isotropic, 1470 uA, 68 kV, XtremeCT II Scanco Medical AG, Brüttisellen, Switzerland) with the same titanium rod inserted into the fully drilled tunnel.

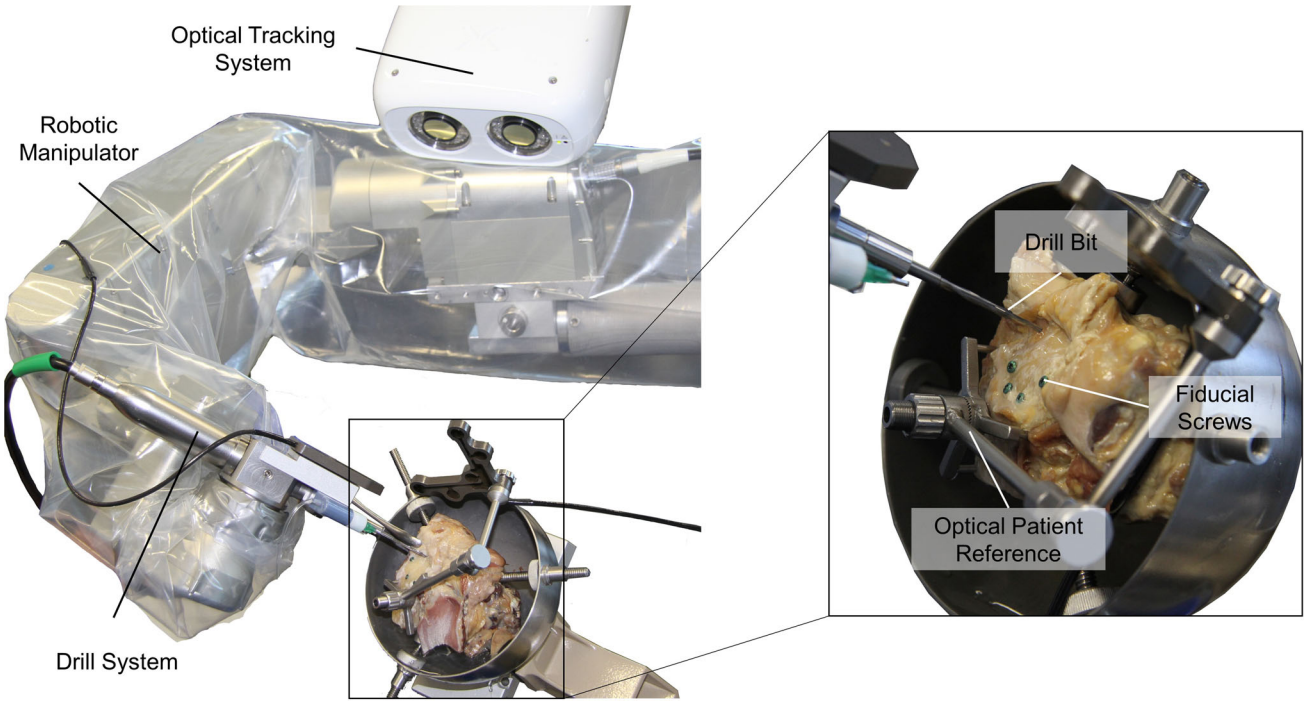

Fig. 4 Experimental setup. Robotic system with optical tracking and drill system. Rigidly clasped temporal bone sample with four fiducial titanium screws and the attached patient optical reference

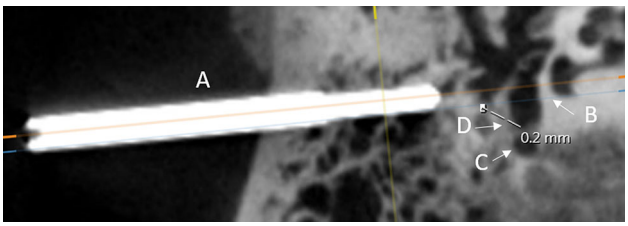

Fig. 5 Manual analysis of the predicted facial nerve safety margin involves. **a** Reslicing of the image along the titanium rod. **b** Propagation of the edge of the rod. **c** Locating the facial nerve. **d** Calculating the distance from the facial nerve

Within the high-resolution postoperative image sets, the inserted titanium rod was segmented using thresholding with manual corrections and the facial nerve was segmented manually by a clinical expert using commercially available software (Amira, Thermo Scientific™, USA. Facial nerve proximity was calculated as the closest distance between these segmented structures (Amira, Thermo Scientific™, USA). To determine the drilling accuracy, preoperative and postoperative image data were coregistered using a normalized mutual information algorithm. The axis of the segmented rod was determined using principle component analysis (MATLAB, Mathworks, USA) and drilling error calculated as the Euclidean distance between the postoperative rod axis and axis of the preoperatively planned trajectory at the depth of the planned target on the round window membrane.

Accuracy assessment

The postoperatively measured distances were compared to those determined intraoperatively: manual and computer-assisted facial nerve proximity calculations and computer-assisted drilling error. The accuracy of the manual and computer-assisted facial nerve proximity calculations was compared using a t test with significance level $P < 0.05$.

Unlike manual analysis, the presented computer-assisted approach relies on the preoperative anatomy segmentation for a proximity measure. To assess the accuracy of the computer-assisted facial nerve proximity prediction algorithm, independent of preoperative facial nerve segmentation accuracy, an accuracy evaluation relative to the preoperatively segmented facial nerve was also conducted. The preoperatively segmented facial nerve was aligned to the high-resolution postoperative image data using normalized mutual information alignment of the preoperative and postoperative image datasets. The distance from the manually segmented rod in the postoperative image dataset and the aligned preoperatively segmented facial nerve was calculated and compared to values obtained using the intraoperative computer-based approach.

Results

RCI access trajectories were planned in 23 cases with margins to the facial nerve ranging from 0.01 to 0.58 mm. All 23 specimens were successfully prepared and drilled using the described system. Visual inspection of intraoperative CBCT images confirmed sufficient image quality to distinguish the inserted titanium rod, fiducial screws and surrounding tissue in all cases (Fig. 6). In two cases, the titanium rod was insufficiently inserted into the drilled tunnel to allow postoperative analysis (the rod did not reach the depth of the facial nerve). This led to exclusion of the data from further analysis. An additional two cases were excluded due to unexplained insufficient imaging quality in the postoperative image dataset (insufficient signal resulting in a low contrast, noisy and hollow representation of the rod), which prevented a sufficiently accurate segmentation of the rod for postoperative analysis. The accuracy of the manual and computer-assisted safety analysis was calculated for the remaining 19 cases.

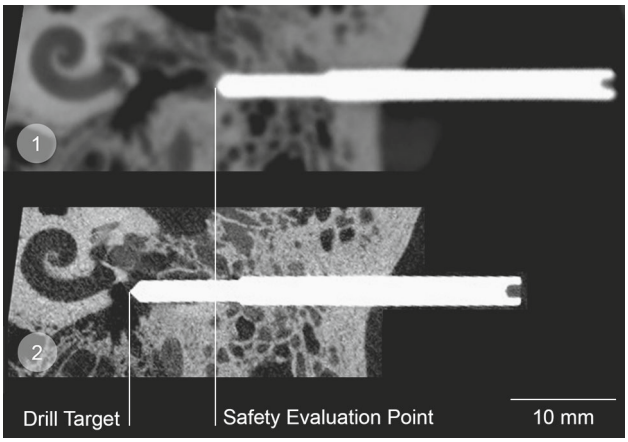

Fig. 6 Intraoperative CBCT image used for safety analysis (acquired 3 mm before the facial nerve, 0.3 mm isotropic resolution), above (1), and postoperative high-resolution CT image of the completely drilled tunnel (0.06 mm isotropic resolution), below (2). Both images acquired with the titanium rod inserted in the drilled tunnel

In each case, only one intraoperative CBCT image dataset was acquired to achieve successful analysis. To reduce the likelihood of requiring an additional scan, two-dimensional scout images were acquired prior to acquisition of the full volume to confirm all required structures were positioned in the imaging volume.

Compared to postoperatively calculated distances, the accuracy of intraoperative facial nerve proximity prediction measurements calculated by the presented computer-assisted approach was 0.22 ± 0.15 mm (median: 0.21, min: 0.02, maximum: 0.61 mm). The accuracy of the drilling error prediction was 0.11 ± 0.08 mm (median: 0.08, min: 0.01, max: 0.3 mm). The time taken to perform each computer-assisted safety analysis was approximately 40 s.

The error associated with the manual prediction of facial nerve proximity was significantly higher ($P = 0.038$) at 0.34 ± 0.20 mm (median: 0.31, min: 0.02, maximum: 0.71 mm) (Fig. 7). Manual assessment required approximately 30 min for each case.

In all cases except two, for both the computer-based and manual calculation, predicted distances were less than the postoperatively determined distances and thus safety margins were underestimated. In the two remaining cases, the error in the predicted distance was negligible with the safety margin being overestimated with an accuracy of 0.02 mm.

When verified against the preoperatively segmented facial nerve (accuracy of the computerized analysis independent of preoperative facial nerve segmentation accuracy), the presented computerized approach predicted the facial nerve

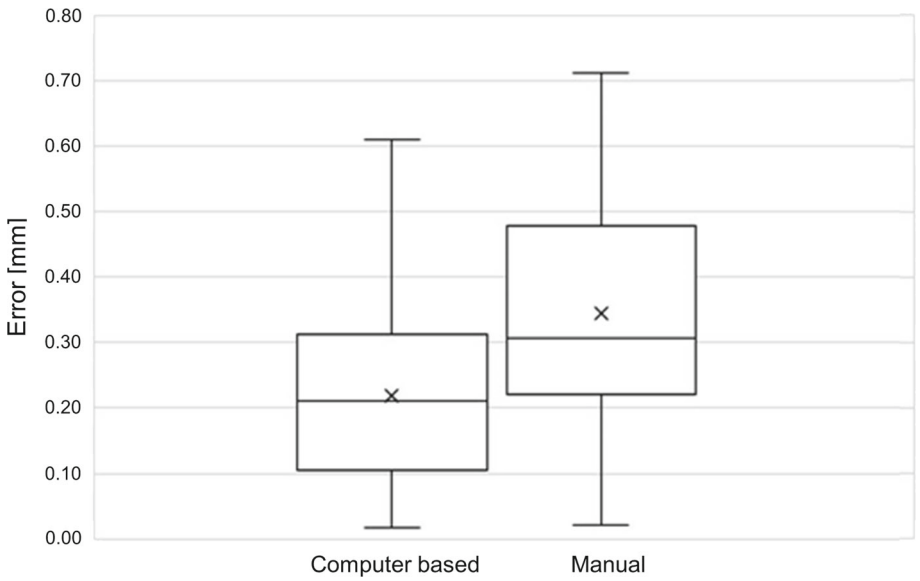

Fig. 7 Nerve proximity prediction error distributions: computer-based versus manual prediction for $N = 19$ intraoperative assessments during RCI procedures on temporal bone specimens

proximity with an accuracy of 0.05 ± 0.05 mm (median: 0.03, min: 0.00, maximum: 0.15 mm).

Discussion

Robotic cochlear implantation poses potential benefits over the traditional surgical approach such as reduced invasiveness and optimized electrode placement. However, to ensure preservation of the facial nerve in case of unexpected navigation errors, methods to determine nerve proximity of the drill tunnel are required. In the case of intraoperative detection of insufficient drilling distance to the facial nerve, or expectantly high drilling error, the surgery can be reverted to a conventional mastoidectomy and posterior tympanotomy approach through the facial recess.

Intraoperative imaging enables the drill tunnel location to be determined independently of navigation errors prior to reaching a critical drilling depth. However, without a clear understanding of the error associated with image-based analysis, the surgeon's ability to successfully apply and trust the safety analysis is greatly diminished. Additionally, with the proposal and implementation of multiple intraoperative safety mechanisms, challenges pertaining to possible conflicting safety measures arise. Deciding which mechanism to trust or implementation of a successful data fusion algorithm requires an understanding of the associated uncertainty in the safety measurements. Within this work, the accuracy of manual and computer-assisted image-based safety analysis of RCI has been evaluated for the first time. Results of the presented study suggest that a computer-assisted image-based analysis provides a valuable assessment of procedure safety, providing greater accuracy drill tunnel localization than a force–density correlation-based assessment. While manual analysis enables measurements to be conducted independently of preoperative anatomy segmentation, the associated accuracy was significantly less than that achieved with a computer-based approach and the time to perform the analysis was significantly more.

Image-based accuracy assessment for RCI poses certain challenging requirements with respect to the quality of the available intraoperative imaging and the ability to assess submillimeter distances on the acquired data. Within the presented study, the manual intraoperative assessment of image data was performed by a single neuroradiologist specially trained and experienced in performing such an image-based analysis for RCI. While subpixel measurement accuracies could be achieved in some cases, the approach was unsurprisingly associated with a greater variance in measurement accuracy. As in the computerized approach, estimated distances were mostly underestimated, resulting in smaller safety margin estimations. This effect may be due to the user performing clinically cautious measurements. While error in this direction does not place the facial nerve at risk, it could result in the robot procedure being aborted unnecessarily. It is important to note that the direction of the error relative to the drill tunnel may vary between users. In the future, evaluation of inter- and intra-user variability would provide a more significant analysis of the error associated with manual analysis.

Automation of the image assessment eliminates effects of user variability and enables subpixel structure delineation and distance calculations. While variability in image quality is common, the presented algorithms demonstrated robustness against changes in intensity of the titanium rod due to normal variation observed in CBCT images. The use of a general threshold value for rod and screw segmentation did not pose a problem over the included CBCT datasets. Application of an accurate fiducial-based pre-alignment of the image data during analysis meant that image intensities corresponding to the titanium rod in the intraoperative image did not have to be excluded from the mutual information registration. Basing analysis on an inserted titanium rod rather than the tunnel itself provided greater contrast of the tunnel in the image and enabled high-accuracy measurements. It must, however, be noted that any unexpected increase in drill hole diameter due to run out of the drill or inaccurately sized drill bits may place the facial nerve at risk and would not be detected using the presented methodology.

When compared to postoperative analysis independent of facial nerve segmentation (utilizing the preoperative facial nerve segmentation for analysis), the presented computer-based approach demonstrated very high accuracy (0.05 mm). However, this accuracy was reduced when compared to postoperative segmentations of the facial nerve (0.22 mm). This discrepancy in error is most likely attributed to oversegmentation of the facial nerve from the preoperative CT (Fig. 8). Oversegmentation has been previously advocated in order to protect the facial nerve and may also be a natural result of the utilized segmentation algorithms and user caution [8]. Again this oversegmentation, while increasing error and uncertainty in the measurement, does not place the facial nerve at risk. It may, however, lead to the classification of a safe drill trajectory as unsafe and thus limits the distance at which trajectories can be planned to the facial nerve. Alternatively, methods for more accurate and precise segmentation of the facial nerve would aid not only in reducing the uncertainty in a computer-assisted image-based assessment of the procedure safety, but also benefit surgical planning and procedure inclusion rates [11]. Automated facial nerve boundary detection algorithms that aim to eliminate user variation and provide a more accurate segmentation are currently under investigation [13].

RCI segmentation and planning is currently performed on image data acquired with helical CT [1]. While CBCT has been associated with benefits for intraoperative imaging

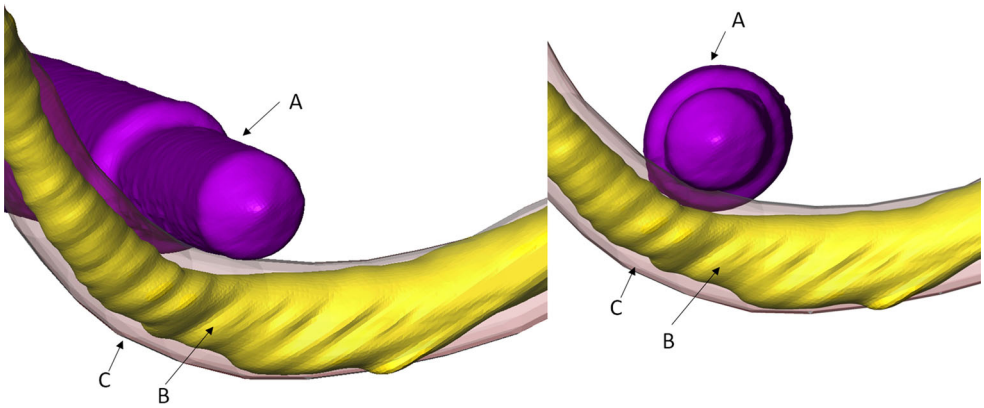

Fig. 8 Effect of facial nerve oversegmentation on the accuracy of the computerized intraoperative image-based safety analysis with **a** segmented drill tunnel from postoperative image data (titanium rod), **b** segmented facial nerve from postoperative image data, **c** overlaid preoperatively segmented facial nerve used in the intraoperative distance calculation

(reduced dose [14, 15], reduced metallic artifacts, portability, high geometric resolution), it may also exhibit higher levels of noise, geometric distortion and variations in signal [16]. In this study, the quality of the CBCT images of the temporal bone specimens was determined sufficient for use with the presented computer-assisted analysis. Imaging results may, however, vary for whole head specimens. CBCT is an uncalibrated imaging modality, and intensities pertaining to a particular material vary depending on system exposure parameters and location of the material within the imaged sample [17]. While this study has demonstrated robustness across image intensity variations associated with a single CBCT imaging system and similar samples, it is suggested that image parameters threshold values in the presented computer-based analysis be optimized when utilizing a different imaging system or sample size. To verify the effect of these variations on the presented algorithms and on manual assessment of the image data, further evaluation is required.

The use of a computer-assisted analysis of image data based on the preoperative plan additionally enables the intraoperative calculation of alternative safety metrics. While the presented evaluation is specific to the preservation of the facial nerve, the methodology could be applied to other structures, segmented preoperatively (e.g., chorda tympani, ossicles) with equal effectiveness. Additionally, as demonstrated in the results of this study, the drilling accuracy and target error can also be predicted with subpixel accuracy. An unexpected high drilling error is of interest independently of anatomy proximity as it may be indicative of a greater technical problem or may affect the site of electrode insertion.

Results of this study demonstrate the accuracy of image-based assessment at predicting facial nerve proximity prior to reaching a critical drilling depth. This would ensure protection against not only mechanical damage but also thermal damage which may result from drilling too close to the nerve tissue. Additionally, in contrast to force-based methods [4], image-based safety analysis is minimally effected by anatomical variation and therefore exhibits greater reliability in measurement. Unlike force-based methods, the image-based approach is not expected to be effected by ossification of the mastoid because the methodology relies on the detection of the inserted rod only and is relatively independent of surrounding structures. However, despite its benefits, intraoperative imaging-based assessment is associated with additional resource costs (specialist personnel, procedural time) that must be considered in addition to patient irradiation dose. Preliminary experience from an ongoing clinical trial suggests that the overall time for an intraoperative CBCT acquisition and image-based safety analysis requires 45–60 min [1]. This time estimation is based on first clinical cases and includes the removal of the dynamic reference base, patient positioning, draping, image acquisition, reconstruction and analysis. While this value is likely to decrease with experience, the additional cost may be deemed unacceptable in a procedure which is traditionally performed in 1.5–3 h. Thus, further investigation into the necessity of image-based safety analysis is required. A likely future implementation is the consistent reliance on less resource-intensive neuromonitoring and force-based methods unless indication of uncertainty in the safety measurement.

Funding This study was funded by the Commission for Technology and Innovation KTI, Switzerland (176181).

Compliance with ethical standards

Conflict of interest The authors declare that they have no conflict of interest.

Ethical approval The ex vivo study was approved by the local institutional review board (KEK-BE 2016-00887).

References

1. Caversaccio M, Gavaghan K, Wimmer W, Williamson T, Ansò J, Mantokoudis G, Gerber N, Rathgeb C, Feldmann A, Wagner F, Scheidegger O, Kompis M, Weisstanner C, Zoka-Assadi M, Roesler K, Anschuetz L, Huth M, Weber S (2017) Robotic cochlear implantation: surgical procedure and first clinical experience. Acta Otolaryngol 6489(March):1–11
2. Weber S, Gavaghan K, Wimmer W, Williamson T, Gerber N, Anso J, Bell B, Feldmann A, Rathgeb C, Matulic M, Stebinger M, Schneider D, Mantokoudis G, Scheidegger O, Wagner F, Kompis M, Caversaccio M (2017) Instrument flight to the inner ear. Sci Robot 2(4):eaal4916
3. Bell B, Stieger C, Gerber N, Arnold A, Nauer C, Hamacher V, Kompis M, Nolte L, Caversaccio M, Weber S (2012) A self-developed and constructed robot for minimally invasive cochlear implantation. Acta Otolaryngol 132(4):355–360. https://doi.org/10.3109/00016489.2011.642813
4. Williamson TM, Bell BJ, Gerber N, Salas L, Zysset P, Caversaccio M, Weber S (2013) Estimation of tool pose based on force-density correlation during robotic drilling. IEEE Trans Biomed Eng 60(4):969–976
5. Ansó J, Dür C, Gavaghan K, Rohrbach H, Gerber N, Williamson T, Calvo EM, Balmer TW, Precht C, Ferrario D, Dettmer MS, Rösler KM, Caversaccio MD, Bell B, Weber S (2016) A neuromonitoring approach to facial nerve preservation during image-guided robotic cochlear implantation. Otol Neurotol 37(1):89–98
6. Labadie RF, Balachandran R, Noble JH, Blachon GS, Mitchell JE, Reda FA, Dawant BM, Fitzpatrick JM (2013) Minimally invasive image-guided cochlear implantation surgery: first report of clinical implementation. Laryngoscope 124:1–8
7. Bell B, Gerber N, Williamson T, Gavaghan K, Wimmer W, Caversaccio M, Weber S (2013) In vitro accuracy evaluation of image-guided robot system for direct cochlear access. Otol Neurotol 34(7):1284–1290
8. Gerber N, Bell B, Gavaghan K, Weisstanner C, Caversaccio MD, Weber S (2014) Surgical planning tool for robotically assisted hearing aid implantation. Int J Comput Assist Radiol Surg 9(1):11–20
9. Gerber N, Gavaghan KA, Bell BJ, Williamson TM, Weisstanner C, Caversaccio M-D, Weber S (2013) High-accuracy patient-to-image registration for the facilitation of image-guided robotic microsurgery on the head. IEEE Trans Biomed Eng 60(4):960–968
10. Studholme C (1997) Measures of 3D medical image alignment. PhD thesis, University of London, London
11. Williamson T, Gavaghan K, Gerber N, Weder S, Anschuetz L, Wagner F, Weisstanner C, Mantokoudis G, Caversaccio M, Weber S (2017) Population statistics approach for safety assessment in robotic cochlear implantation. Otol Neurotol 38(5):759–764
12. Feldmann A, Wandel J, Zysset P (2016) Reducing temperature elevation of robotic bone drilling. Med Eng Phys 38(12):1495–1504
13. Chu C, Geber N, Gavaghan K, Zheng G (2016) Automated facial nerve segmentation : a validation study. In: CURAC, Deutsche Gesellschaft für Computer- und Roboterassistierte Chirurgie, pp 135–136
14. McCollough CH, Bushberg JT, Fletcher JG, Eckel LJ (2015) Answers to common questions about the use and safety of CT scans. Mayo Clin Proc 90(10):1380–1392
15. Xoran Technologies LLC (2017) xCAT IQ user manual
16. Lechuga L, Weidlich GA (2016) Cone beam CT vs. fan beam CT: a comparison of image quality and dose delivered between two differing CT imaging modalities. Cureus 8:e778
17. Elstrøm UV, Muren LP, Petersen JBB, Grau C (2011) Evaluation of image quality for different kV cone-beam CT acquisition and reconstruction methods in the head and neck region. Acta Oncol (Madr) 50(6):908–917